ChemPubSoc Europe
DOI: 10.1002/chem.201304480
CHEMISTRY
A European Journal
Full Paper

Cluster Compounds

A Microporous Anionic Metal–Organic Framework for Sensing Luminescence of Lanthanide(III) Ions and Selective Absorption of Dyes by Ionic Exchange

Jun-Sheng Qin,[a, b] Shu-Ran Zhang,[b] Dong-Ying Du,[b] Ping Shen,[b] Shao-Juan Bao,[b] Ya-Qian Lan,*[c] and Zhong-Min Su*[a, b]

Abstract: Herein, a novel anionic framework with primitive centered cubic (pcu) topology, $[(CH_3)_2NH_2]_4$-$[(Zn_4dttz_6)Zn_3]\cdot 15\,DMF\cdot 4.5\,H_2O$, (**IFMC-2**; $H_3dttz = 4,5$-di(1*H*-tetrazol-5-yl)-2*H*-1,2,3-triazole) was solvothermally isolated. A new example of a tetranuclear zinc cluster $\{Zn_4dttz_6\}$ served as a secondary building unit in **IFMC-2**. Furthermore, the metal cluster was connected by Zn^{II} ions to give rise to a 3D open microporous structure. The lanthanide(III)-loaded metal–organic framework (MOF) materials **Ln^{3+}@IFMC-2**, were successfully prepared by using ion-exchange experiments owing to the anionic framework of **IFMC-2**. Moreover, the emission spectra of the as-prepared **Ln^{3+}@IFMC-2** were investigated, and the results suggested that **IFMC-2** could be utilized as a potential luminescent probe toward different Ln^{3+} ions. Additionally, the absorption ability of **IFMC-2** toward ionic dyes was also performed. Cationic dyes can be absorbed, but not neutral and anionic dyes, thus indicating that **IFMC-2** exhibits selective absorption toward cationic dyes. Furthermore, the cationic dyes can be gradually released in the presence of NaCl.

Introduction

Metal–organic frameworks (MOFs) are the focus of increasing interest owing to not only their structural and chemical diversities but their potential structure-related applications, for instance, gas storage and separation, luminescence, catalysis, and drug delivery.[1,2] Generally, MOFs are assembled in “one-pot” solvothermal or hydrothermal syntheses by judicious selection of metal ions, organic linkers, and the synthetic conditions. In recent years, several MOF materials, consisting of discrete metal-cluster vertices interconnected by organic molecules as linkers, have been designed and synthesized.[3,4] In most cases, the metal-cluster vertices generated in situ act as secondary building units (SBUs) and further extend to multidimensional structures by functionalized organic ligands or metal–organic fragments. This approach is considered to be promising to construct MOFs with specific functionalities or topologies. Moreover, the framework charge (i.e., cationic, neutral, or anionic) of MOF materials also has a great impact on their performance because charged MOFs are typically able to undergo postsynthetic modification by means of ion exchange.[5]

Recently, porous MOF materials with the abilities of absorption and separation toward pollutants, such as dye molecules or metal ions, have been applied in several fields,[6] for instance, the capture of harmful dyes or noxious metal ions, the purification of water, and the inclusion of large biomolecules. Xu and co-workers reported a mesoporous MOF which was employed as a liquid-chromatographic stationary phase for large-molecule separation.[7a] Later, they described another example of column-chromatographic filler for the separation of large dye molecules motivated by the existing large cages.[7b] However, only a few MOFs have been used to absorb or separate dye molecules, and in most cases, dye removal is on the basis of the size-exclusion effect.[7] So far, it is still a challenge to prepare porous charged MOFs used to absorb/separate large molecules or ions by virtue of ionic selectivity.[8]

On the other hand, continuous effort has been dedicated to the design and preparation of multifunctional luminescent MOF materials. Among the reported luminescent materials, lanthanide-containing MOF materials have received exceptional attention owing to the advantages of the ease of design, which allows narrow-band and fine-tuned luminescent properties.[9] Generally, lanthanide-based luminescent MOF materials can be divided into two groups: 1) Ln^{3+} ions directly bonded to the organic linkers/sensitizers to generate MOFs[10] and

---

[a] Dr. J.-S. Qin, Prof. Z.-M. Su
State Key Laboratory of Supramolecular Structure and Materials
Jilin University, Changchun 130012 (P.R. China)
E-mail: zmsu@nenu.edu.cn

[b] Dr. J.-S. Qin, Dr. S.-R. Zhang, Dr. D.-Y. Du, P. Shen, S.-J. Bao, Prof. Z.-M. Su
Institute of Functional Material Chemistry
Faculty of Chemistry, Northeast Normal University
Changchun 130024 (P.R. China)

[c] Prof. Y.-Q. Lan
Jiangsu Key Laboratory of Biofunctional Materials
College of Chemistry and Materials Science
Nanjing Normal University, Nanjing 210023 (P.R. China)
E-mail: yqlan@njnu.edu.cn

Supporting information for this article is available on the WWW under http://dx.doi.org/10.1002/chem.201304480.

2) Ln^{3+} ions encapsulated into porous MOFs by means of postsynthetic modification.[11] Up until now, the preparation and investigation of tuneable luminescent lanthanide–MOF materials has turned out to be a prominent topic in fluorescent materials science.[12] Most of the fluorescent lanthanide–MOF materials, as reported, are available by changing the ratio of Ln^{3+} ions to achieve tuneable fluorescence. However, rare-earth fluorescent probes with similar contents of Ln^{3+} ions are rarely reported, especially the encapsulation of Ln^{3+} ions by the postsynthetic modification of MOFs. It is an issue worthy of study in the field of fluorescent materials.

In our previous report, the zeolite-like neutral MOF with sodalite topology **IFMC-1** (IFMC = Institute of Functional Material Chemistry) has been solvothermally isolated, which exhibits high CO_2 uptake and selective CO_2/N_2 adsorption owing to the favorable interactions between abundant uncoordinated N atoms from aromatic ligands and CO_2 molecules.[13] As a continuation of our work, Zn^{2+} ions and 4,5-di(1*H*-tetrazol-5-yl)-2*H*-1,2,3-triazole (H_3dttz) were employed again, but in DMF media. Fortunately, the anionic framework with a pcu topology $[(CH_3)_2NH_2]_4[(Zn_4dttz_6)Zn_3]\cdot 15\,DMF\cdot 4.5\,H_2O$ (**IFMC-2**) was successfully obtained (Scheme 1). Furthermore, the luminescence of Ln^{3+} ions encapsulated into microporous **IFMC-2** and the absorption of cationic dyes through ion exchange was also carried out. Interestingly, **IFMC-2** exhibited sensing luminescence toward different Ln^{3+} ions and can selectively absorb cationic molecules relative to neutral and anionic molecules due to its anionic framework.

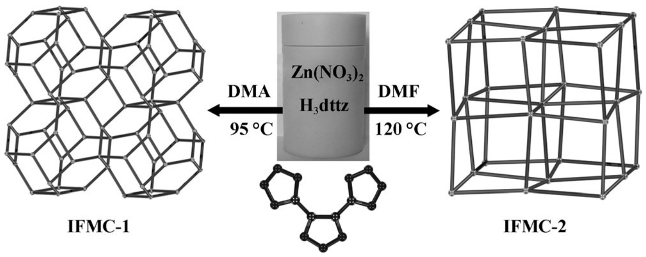

Scheme 1. Schematic view of comparative synthesis for **IFMC-1** and **-2**.

Results and Discussion

A solvothermal reaction of $Zn(NO_3)_2\cdot 6\,H_2O$ and H_3dttz in DMF yields pale-yellow cubic block crystals **IFMC-2**. The formula of **IFMC-2** $[(CH_3)_2NH_2]_4[(Zn_4dttz_6)Zn_3]\cdot 15\,DMF\cdot 4.5\,H_2O$ was elucidated by single-crystal X-ray diffraction studies, thermogravimetric analysis (TGA; see Figure S1 in the Supporting Information), elemental analysis, and charge-balance considerations. Single-crystal X-ray diffraction studies revealed that **IFMC-2** crystallizes in the cubic space group *I*-43*m* (see Table S1 in the Supporting Information). The framework is composed of three types of Zn^{2+} ion and two types of $dttz^{3-}$ fragment (Figure 1 a). The Zn(1) atom adopts a octahedral geometry, which is finished by six nitrogen atoms from six distinct $dttz^{3-}$ ions. The Zn(2) atoms are surrounded by six nitrogen atoms from three different $dttz^{3-}$ ligands and show a distorted-octahedral geometry. In addition, the Zn(3) atom is completed by four nitrogen atoms from two $dttz^{3-}$ moieties and exhibits a distorted-tetrahedral geometry. The Zn–N bond lengths are all within the normal ranges.[13] The Zn(1) and Zn(2) centers are connected to each other by six deprotonated $dttz^{3-}$ ligands to give rise to a tetranuclear zinc cluster (Figure 1 b). This tetranuclear zinc cluster exhibits a tetrahedral structure, which is similar but different from the reported pentanuclear metal cluster (see Figure S2 a, b in the Supporting Information).[4] In the pentanuclear metal cluster, four Zn^{2+} ions are located at each vertex of the regular tetrahedron and the fifth Zn^{2+} ion resides in the center, whereas one Zn^{2+} ion at vertex of the tetrahedron is missing in this tetranuclear zinc cluster. It should be noted that this example of a tetranuclear metal cluster is new relative to the previously reported clusters (see Figure S2 c in the Supporting Information).[3a] Moreover, the tetranuclear cluster was extended by Zn(3) ions to result in a 3D non-interpenetrating open framework with two types of channel structure (see Figure 1 c and Figure S3 in the Supporting Information). Furthermore, the two types of channel can be divided into only one type of cubic cage structure (see Figure S4 in the Supporting Information). The distance between two adjacent tetranuclear zinc clusters is approximately 15 Å and the open size of cage is approximately 10 Å, thus suggesting a microporous characteristic of **IFMC-2**. Overall, the framework of **IFMC-2** is anionic, which is filled with $[(CH_3)_2NH_2]^+$ ions and guest molecules. The protonated $[(CH_3)_2NH_2]^+$ ions in **IFMC-2** originate from the decarbonylation of dimethylamine.[14] Given the charge-balance consideration, there are four $[(CH_3)_2NH_2]^+$ ions per formula unit. However, the disordered cations and guest molecules are not crystallographically well defined. PLATON calculations[15] suggest that the solvent-accessible volume in **IFMC-2** is about 20221.3 $Å^3$ per unit cell (71.3 % of the cell volume).

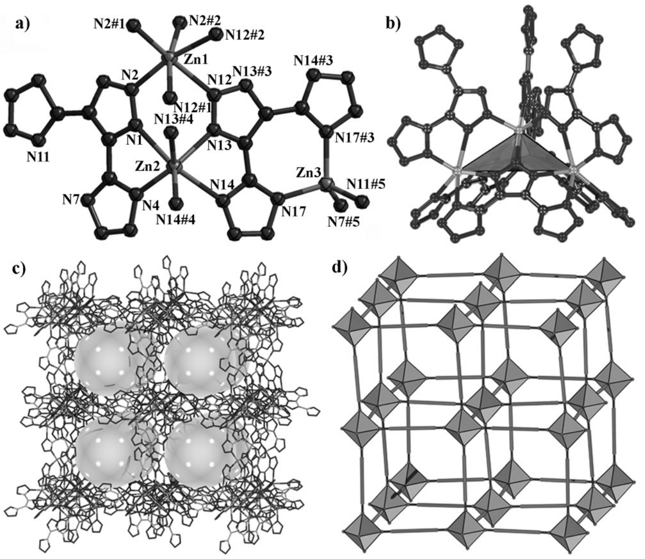

Figure 1. The structure of **IFMC-2**. a) The coordination environments of Zn^{2+} ions, #1 1−*y*, 1−*z*, *x*; #2 *z*, 1−*x*, 1−*y*; #3 *z*, *y*, *x*; #4 1−*y*, 1−*x*, *z*; #5 0.5−*x*, 1.5−*z*, −0.5+*y*; b) the tetranuclear metal cluster; c) the 3D open framework, and d) the pcu topology.

To study the structure further, if each tetranuclear cluster is considered as a six-connected node and the Zn(3) cations as linkers, the structure can be regarded as a distorted pcu topology (Figure 1 d).[16] In **IFMC-2**, the two tetrazolate rings are almost parallel to the triazolate plane, whereas the dihedral angles between the triazolate and tetrazolate rings are approximately 29.85 and 27.49°, respectively, and the dihedral angle of the two tetrazolate rings is approximately 43.69° in **IFMC-1**. The reason for the formation of different cage structures and topologies of **IFMC-1** and **-2** (see Figure S5 in the Supporting Information and Scheme 1) perhaps results from the different coordination modes of the Zn^{2+} ions and the distortion degree of the $dttz^{3-}$ ligands.

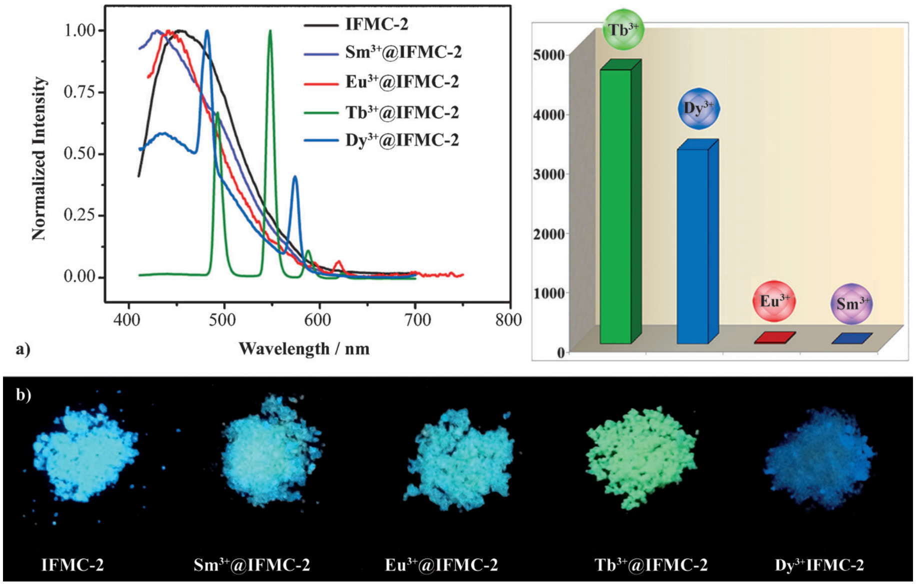

Figure 2. a) Emission spectra of **IFMC-2**, **Sm^{3+}@IFMC-2**, **Eu^{3+}@IFMC-2**, **Tb^{3+}@IFMC-2**, and **Dy^{3+}@IFMC-2** in the solid state at room temperature (left), and the peak intensities of the highest characteristic peak of Sm^{3+}, Eu^{3+}, Tb^{3+}, and Dy^{3+} in their emission spectra (right). b) Samples illuminated with laboratory UV light ($\lambda_{ex}=254$ nm).

The preparation of luminescence materials with lanthanide cations encapsulated within the MOF pores is currently of interest in the fields of light display, lasers, and optoelectronic devices. As a matter of fact, the anionic framework of **IFMC-2** makes a chance and is a driving force for cation-exchange experiments, in which the $[(CH_3)_2NH_2]^+$ ions perhaps could be exchanged with lanthanide cations. In this sense, we tried to load lanthanide ions into the cavity of **IFMC-2** and then analyze the luminescent properties of the resulting **Ln^{3+}@IFMC-2** ($Ln^{3+}=Sm^{3+}$, Eu^{3+}, Tb^{3+}, or Dy^{3+}). To introduce lanthanide ions into the cavities of **IFMC-2**, fresh-prepared **IFMC-2** was soaked in solutions of the nitrate salts of Sm^{3+}, Eu^{3+}, Tb^{3+}, or Dy^{3+} in DMF to yield **Sm^{3+}@IFMC-2**, **Eu^{3+}@IFMC-2**, **Tb^{3+}@IFMC-2**, or **Dy^{3+}@IFMC-2**, respectively. The exchanged samples were collected by filtration after 48 hours, washed with DMF for several times until no characteristic emission was observed upon excitation, and then dried in air. The porous network of **IFMC-2** was almost unchanged after the encapsulation of Ln^{3+} ions, as confirmed by X-ray powder diffraction patterns (XRPD; see Figure S6 in the Supporting Information).[17] From the evidence of the IR spectra (see Figures S7 and S8 in the Supporting Information) combined with the XRPD patterns, we consider that their basic frameworks are still maintained. Accordingly, the inductively coupled plasma (ICP) data (see Table S2 in the Supporting Information) for **Ln^{3+}@IFMC-2** isolated after immersion in solutions of Ln^{3+} ions in DMF for 48 h suggests that similar encapsulation amounts of Ln^{3+} (Sm^{3+}, Eu^{3+}, Tb^{3+}, or Dy^{3+}) ions were absorbed into **IFMC-2**. The molar ratio of Zn^{2+}/Ln^{3+} is approximately 21:1, which means that one $[(CH_3)_2NH_2]^+$ ion was exchanged by 0.33 Ln^{3+} ions per unit.

Clusters **Sm^{3+}@IFMC-2**, **Eu^{3+}@IFMC-2**, and **Dy^{3+}@IFMC-2** display very similar emissions but different intensities with **IFMC-2** ($\lambda_{ex}=374$ nm) and cover the range $\lambda=400$–500 nm (Figure 2 a). In addition, no characteristic emission was observed for **Sm^{3+}@IFMC-2**. In terms of **Eu^{3+}@IFMC-2**, a much weaker characteristic emission of the Eu^{3+} ion at $\lambda_{em}=619$ nm appears upon excitation at $\lambda_{ex}=395$ nm.[18a,b] Interestingly, the **Tb^{3+}@IFMC-2** sample emits its distinctive green color when excited at $\lambda_{ex}=279$ nm, which originated from the characteristic transitions of $^5D_4\rightarrow{}^7F_J$ ($J=3$–6) of the Tb^{3+} ions.[18b] Two intense emission bands at $\lambda_{em}=493$ and 548 nm originate from the $^5D_4\rightarrow{}^7F_6$ and $^5D_4\rightarrow{}^7F_5$ transitions, whereas the weaker emission bands at $\lambda_{em}=588$ and 624 nm correspond to the $^5D_4\rightarrow{}^7F_4$ and $^5D_4\rightarrow{}^7F_3$ transitions. The **Dy^{3+}@IFMC-2** cluster is blue luminescent in the solid state with typical Dy^{3+} emissions at $\lambda_{em}=482$ and 574 nm, which correspond to the characteristic emission $^4F_{9/2}\rightarrow{}^6H_J$ transitions of the Dy^{3+} ions ($J=15/2$ and 13/2).[18c] Additionally, the blue emission of the $^4F_{9/2}\rightarrow{}^6H_{15/2}$ transition has a stronger intensity than the yellow emission of the $^4F_{9/2}\rightarrow{}^6H_{13/2}$ transition. It should be noted that the luminescence intensity of **Tb^{3+}@IFMC-2** is beyond the detection limitation when determined under the photomultiplier tube (PMT) voltage of 700 V (excitation slit: 2.5 nm, emission slit: 2.5 nm). In this context, the luminescence of the **Tb^{3+}@IFMC-2** sample was measured with the PMT voltage of 500 V, whereas the other samples were measure with the PMT voltage of 700 V. Even under these conditions, the emission intensity of the highest characteristic peak of **Tb^{3+}@IFMC-2** ($\lambda_{em}=548$ nm, 4606) is much higher than those of **Dy^{3+}@IFMC-2** ($\lambda_{em}=482$ nm, 3266), and **Eu^{3+}@IFMC-2** ($\lambda_{em}=619$ nm, 22). These results suggest that although the encapsulation amounts of Ln^{3+} ions are similar for **Sm^{3+}@IFMC-2**, **Eu^{3+}@IFMC-2**, **Tb^{3+}@IFMC-2**, and **Dy^{3+}@IFMC-2**, the emission intensities are greatly different (Figure 2 a, right). Moreover, these results indicate that the microporous **IFMC-2** is suitable for the sensitization of Tb^{3+} and Dy^{3+} ions rather than as a Eu^{3+} and Sm^{3+} emitter. Correspondingly, when illuminated with a standard laboratory UV lamp ($\lambda_{ex}=254$ nm), **Tb^{3+}@IFMC-2** and **Dy^{3+}@IFMC-2** emitted their distinctive green and blue colors, respectively, which were readily observed with the naked eye as a qualitative indication of terbium and dysprosium sensitization (Figure 2b).

Dyes are widely employed in several industries, including paper, textiles, plastics, cosmetics, printing, and pharmaceuticals.[19] As a result, the removal of dyes from effluents before discharge into natural bodies is of great importance from an environmental point of view. To evaluate the absorption ability toward dye molecules, we selected freshly prepared **IFMC-2** to capture dyes from solutions in DMF. According to the pore size of **IFMC-2**, we selected five dyes, including cationic, neutral and anionic dyes, which perhaps would be absorbed. Firstly, the freshly prepared **IFMC-2** was immersed in solutions of dyes in DMF (Figure 3; methylene blue (MB), basic red 2 (BR), crystal violet (CV), solvent yellow 2 (SY), and methyl orange (MO), respectively). The cationic dyes (i.e., MB, BR, and CV) could be absorbed over a period of time and the pale-yellow crystals gradually became coloured, while the neutral and anionic dyes (i.e., SY and MO, respectively) could not be absorbed (Figure 3). The selective absorption of cationic dyes perhaps results from the interaction of the cationic dye molecules and anionic framework of **IFMC-2**. Meanwhile, the abilities of **IFMC-2** to absorb cationic dyes from solutions of DMF were determined through UV/Vis spectroscopic analysis (see Figures S9 and S10 in the Supporting Information). Spectroscopic study of the supernatants indicated that MB was almost completely absorbed into the network of **IFMC-2**, whereas half of BR and CV were left in the supernatants within a certain period of time. The difference in absorption between the three types of dye may be caused by shape and size because MB is linear and BR and CV are planar and BR and CV are relatively larger than MB. Similarly, the successful exchange of cationic dyes does not influence the crystalline integrity of **IFMC-2**, as demonstrated by the XRPD profiles (see Figure S11 in the Supporting Information).[17] The results suggest that **IFMC-2** perhaps is a potential absorbent for the removal of cationic dyes from effluents.

Furthermore, to confirm whether the absorption toward cationic dyes is due to ionic interaction between the cationic dye and anionic framework, dye-releasing experiments were also performed in pure DMF and a saturated solution of NaCl in DMF, respectively. The release process was monitored by using UV/Vis spectroscopy.[20] The results suggest that the dye molecules in **dye@IFMC-2** can be gradually released in the presence of NaCl, whereas the dye molecules are hardly released without NaCl (see Figure 4 and Figure S12 in the Supporting Information). In this case, we can speculate that the absorption can be assigned to the ionic interaction of the dyes with the anionic framework. That is to say, the dye release is an ion-exchange process. Furthermore, the process of dye uptake and release in the presence of NaCl was studied for another two runs (see Figure S13 in the Supporting Information). These results suggest that the dye uptake and release is a reversible process and that the dye can be almost completely released in the presence of NaCl with enough time.

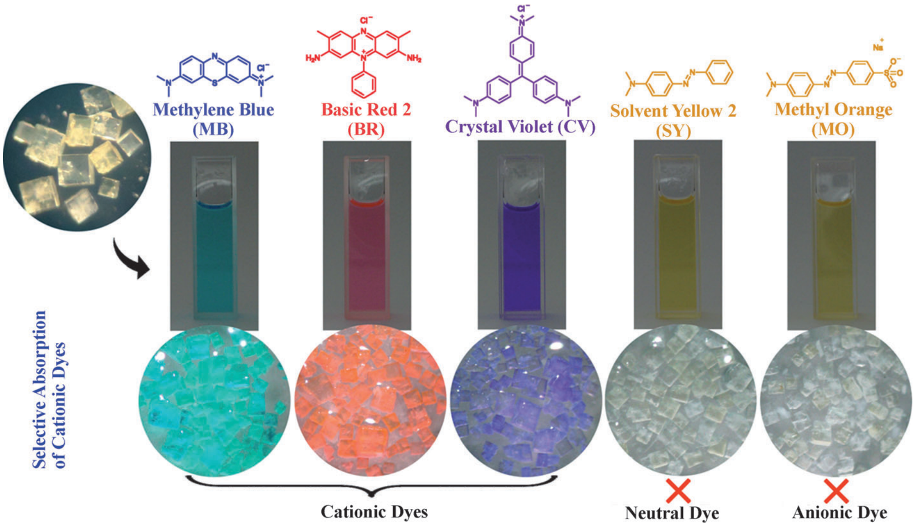

Figure 3. The dye molecules employed in the dye-absorption experiments and photographs of the corresponding crystals after immersion into the solutions of the dyes for a period of time.

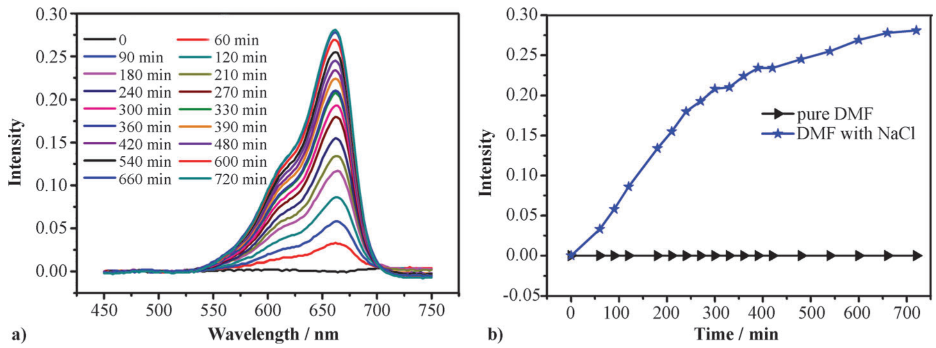

Figure 4. a) The MB released from the **MB@IFMC-2** cluster in a saturated solution of NaCl in DMF monitored by UV absorption; b) the release-rate comparison of MB from **MB@IFMC-2** in pure DMF (black) and a saturated solution of NaCl in DMF (blue).

Conclusion

In summary, a new MOF material with a pcu topology, **IFMC-2**, has been solvothermally synthesized, in which a new example of a tetranuclear zinc cluster $\{Zn_4dttz_6\}$ serves as a SBU. The same precursors react in different solvent systems to result in two MOFs with different topologies and framework charges (**IFMC-1** and **-2**). The Ln^{3+}-loaded MOF materials were successfully prepared by means of cation-exchange experiments. The emission spectra of the as-prepared Ln^{3+}-loaded MOF materials indicated that **IFMC-2** is suitable for the sensitization of Tb^{3+} and Dy^{3+} ions rather than as Eu^{3+} and Sm^{3+} emitters. Furthermore, **IFMC-2** could be employed as a potential luminescent probe toward different Ln^{3+} ions. In addition, the organic cations in **IFMC-2** can be exchanged with cationic dyes owing to the anionic framework. However, neutral and anionic dyes could not be absorbed because **IFMC-2** exhibited selectively absorption ability towards cationic dyes. Moreover, the cationic dyes could be gradually released in the presence of NaCl, thus suggesting that the absorption perhaps results from the virtue of the ionic interaction between the cationic dyes and the anionic framework. Furthermore, the process of the dye uptake and release was reversible. This process makes it possible to separate large molecules with similar sizes but opposite charges. This work opens up a plethora of prepared Ln^{3+}-loaded MOF luminescence materials through encapsulation of Ln^{3+} ions into an anionic framework and the selective absorption of ionic molecules through ionic interactions. Further study into the design and preparation of novel charged MOF materials is ongoing in our laboratory.

Experimental Section

Materials

All the reagents and solvents for the syntheses were purchased from commercial sources and used as received, except for H_3dttz, which was synthesized according to a previous report.[13]

Preparation of IFMC-2

$Zn(NO_3)_2 \cdot 6H_2O$ (0.20 g, 0.67 mmol) was added to a solution of H_3dttz (0.10 g, 0.50 mmol) in DMF (5 mL) with stirring. The mixture was heated at 120 °C for 72 h and then cooled to room temperature. Pale-yellow block crystals were collected and dried in air (yield = 78 %, based on $Zn(NO_3)_2 \cdot 6H_2O$). IR (KBr; Figure S8): $\tilde{\nu} = 3443$ (m), 2931 (m), 1661 (s), 1558 (w), 1493 (m), 1441 (m), 1413 (m), 1388 (s), 1255 (m), 1211 (w), 1168 (w), 1100 (m), 1063 (w), 1023 (w), 1001 (m), 760 (w), 663 (m) cm^{-1}; elemental analysis (%) calcd for $C_{77}H_{146}N_{85}O_{19.5}Zn_7$ (3032.38): C 30.50, H 4.85, N 39.26; found: C 30.78, H 4.71, N 39.47.

X-ray crystallographic analysis

Single-crystal X-ray diffraction data for **IFMC-2** were recorded on a Bruker ApexII CCD diffractometer with graphite-monochromated MoK_α radiation ($\lambda = 0.71073$ Å) at 293 K. Absorption corrections were applied by using the multiscan technique. Its structure was solved by the direct method of SHELXS-97[21a] and refined by full-matrix least-squares techniques using the SHELXL-97 program[21b] within WINGX.[21c] Because guest molecules in the channels of **IFMC-2** were highly disordered and could not be modeled properly, the SQUEEZE routine of PLATON[15] was applied to remove their contributions to the scattering. The reported refinements are of the guest-free structures obtained by the SQUEEZE routine, and the results were attached to the CIF file. CCDC-956905 contains the supplementary crystallographic data for this paper. The data can be obtained free of charge from The Cambridge Crystallographic Data Centre via www.ccdc.cam.ac.uk/data request/cif.

Encapsulation of lanthanide(III) ions in IFMC-2

Freshly prepared **IFMC-2** (50 mg) was soaked in solutions of the nitrate salts of Sm^{3+}, Eu^{3+}, Tb^{3+}, or Dy^{3+} in DMF (2 mL, 0.5 mmol), respectively. After soaking for 2 days, the crystals were washed with DMF several times to remove residual lanthanide(III) cations on the surface.

Dye absorption and release

Dye absorption: Freshly prepared **IFMC-2** (50 mg) was transferred into solutions of Methylene Blue (MB), Basic Red 2 (BR) Crystal Violet (CV), Solvent Yellow 2 (SY), and Methyl Orange (MO) in DMF (2 mL) in cuvettes (4 mL).

Dye release: The **IFMC-2** clusters loaded with MB, BR, and CV (40 mg) were transferred into pure DMF and a saturated solution of NaCl in DMF (2 mL) in cuvettes (4 mL), respectively. UV/Vis spectra were employed to measure the absorption ability and release process of **IFMC-2** after certain time intervals.

Acknowledgements

This work was financially supported by the Pre-973 Program (2010CB635114), the National Natural Science Foundation of China (No. 21001020 and 21371099), the Science and Technology Development Planning of Jilin Province (No. 20140520089JH), and Graduate Innovation Fund of Jilin University (No. 20121048).

Keywords: cluster compounds · dyes/pigments · luminescence · sensors · metal–organic frameworks · zinc

[1] a) K. S. Jeong, Y. B. Go, S. M. Shin, S. J. Lee, J. Kim, O. M. Yaghi, N. Jeong, *Chem. Sci.* **2011**, *2*, 877–882; b) T. Wu, R. Khazhakyan, L. Wang, X. H. Bu, S. T. Zheng, V. Chau, P. Y. Feng, *Angew. Chem.* **2011**, *123*, 2584–2587; *Angew. Chem. Int. Ed.* **2011**, *50*, 2536–2539; c) K. Otsubo, Y. Wakabayashi, J. Ohara, S. Yamamoto, H. Matsuzaki, H. Okamoto, K. Nitta, T. Uruga, H. Kitagawa, *Nat. Mater.* **2011**, *10*, 291–295; d) H.-L. Jiang, B. Liu, T. Akita, M. Haruta, H. Sakurai, Q. Xu, *J. Am. Chem. Soc.* **2009**, *131*, 11302–11303; e) J. R. Li, H.-C. Zhou, *Nat. Chem.* **2010**, *2*, 893–898; f) J.-R. Li, R. J. Kuppler, H.-C. Zhou, *Chem. Soc. Rev.* **2009**, *38*, 1477–1504; g) Y. Chen, G. Li, Z. Chang, Y. Qu, Y. Zhang, X. Bu, *Chem. Sci.* **2013**, *4*, 3678–3682.

[2] a) A. M. Shultz, O. K. Farha, J. T. Hupp, S. T. Nguyen, *J. Am. Chem. Soc.* **2009**, *131*, 4204–4205; b) Y. E. Cheon, M. P. Suh, *Angew. Chem.* **2009**, *121*, 2943–2947; *Angew. Chem. Int. Ed.* **2009**, *48*, 2899–2903; c) B. Chen, S. Xiang, G. Qian, *Acc. Chem. Res.* **2010**, *43*, 1115–1124; d) R. E. Morris, X. Bu, *Nat. Chem.* **2010**, *2*, 353–361; e) D. Du, J. Qin, T. Wang, S. Li, Z. Su, K. Shao, Y. Lan, X. Wang, E. Wang, *Chem. Sci.* **2012**, *3*, 705–710; f) H.-L. Jiang, B. Liu, Y.-Q. Lan, K. Kuratani, T. Akita, H. Shioyama, F. Zong, Q. Xu, *J. Am. Chem. Soc.* **2011**, *133*, 11854–11857.

[3] a) M. Eddaoudi, J. Kim, N. Rosi, D. Vodak, J. Wachter, M. O'Keeffe, O. M. Yaghi, *Science* **2002**, *295*, 469 – 472; b) J. J. Perry IV, J. A. Perman, M. J. Zaworotko, *Chem. Soc. Rev.* **2009**, *38*, 1400 – 1417; c) D. J. Tranchemontagne, J. L. Mendoza-Cortés, M. O'Keeffe, O. M. Yaghi, *Chem. Soc. Rev.* **2009**, *38*, 1257 – 1283; d) D. Du, J. Qin, Z. Sun, L. Yan, M. O'Keeffe, Z. Su, S. Li, X. Wang, X. Wang, Y. Lan, *Sci. Rep.* **2013**, *3*, 2616.

[4] a) Y.-L. Bai, J. Tao, R.-B. Huang, L.-S. Zheng, *Angew. Chem.* **2008**, *120*, 5424 – 5427; *Angew. Chem. Int. Ed.* **2008**, *47*, 5344 – 5347; b) X.-L. Wang, C. Qin, S.-X. Wu, K.-Z. Shao, Y.-Q. Lan, S. Wang, D.-X. Zhu, Z.-M. Su, E.-B. Wang, *Angew. Chem.* **2009**, *121*, 5395 – 5399; *Angew. Chem. Int. Ed.* **2009**, *48*, 5291 – 5295; c) Y.-Q. Lan, S.-L. Li, H.-L. Jiang, Q. Xu, *Chem. Eur. J.* **2012**, *18*, 8076 – 8083.

[5] a) M. Dinca, A. Dailly, J. R. Long, *Chem. Eur. J.* **2008**, *14*, 10280 – 10285; b) Z. Wang, S. M. Cohen, *Chem. Soc. Rev.* **2009**, *38*, 1315 – 1329; c) K. L. Mulfort, O. K. Farha, C. Stern, A. A. Sarjeaut, J. T. Hupp, *J. Am. Chem. Soc.* **2009**, *131*, 3866 – 3868; d) Z. Zhang, W. Shi, Z. Niu, H. Li, B. Zhao, P. Cheng, D. Liao, S. Yan, *Chem. Commun.* **2011**, *47*, 6425 – 6427; e) D.-Y. Du, L.-K. Yan, Z.-M. Su, S.-L. Li, Y.-Q. Lan, E.-B. Wang, *Coord. Chem. Rev.* **2013**, *257*, 702 – 717.

[6] a) H. Deng, S. Grunder, K. E. Cordova, C. Valente, H. Furukawa, M. Hmadeh, F. Gándara, A. C. Whalley, Z. Liu, S. Asahina, H. Kazumori, M. O'Keeffe, O. Terasaki, J. F. Stoddart, O. M. Yaghi, *Science* **2012**, *336*, 1018 – 1023; b) G.-S. Yang, Z.-L. Lang, H.-Y. Zang, Y.-Q. Lan, W.-W. He, X.-L. Zhao, L.-K. Yan, X.-L. Wang, Z.-M. Su, *Chem. Commun.* **2013**, *49*, 1088 – 1090; c) Q. Wen, J. Di, Y. Zhao, Y. Wang, L. Jiang, J. Yu, *Chem. Sci.* **2013**, *4*, 4378 – 4382.

[7] a) H.-L. Jiang, Y. Tatsu, Z.-H. Lu, Q. Xu, *J. Am. Chem. Soc.* **2010**, *132*, 5586 – 5587; b) Y.-Q. Lan, H.-L. Jiang, S.-L. Li, Q. Xu, *Adv. Mater.* **2011**, *23*, 5015 – 5020; c) F. Pu, X. Liu, B. L. Xu, J. S. Ren, X. G. Qu, *Chem. Eur. J.* **2012**, *18*, 4322 – 4328.

[8] C.-Y. Sun, X.-L. Wang, C. Qin, J.-L. Jin, Z.-M. Su, P. Huang, K.-Z. Shao, *Chem. Eur. J.* **2013**, *19*, 3639 – 3645.

[9] a) G. J. He, D. Guo, C. He, X. L. Zhang, X. W. Zhao, C. Y. Duan, *Angew. Chem.* **2009**, *121*, 6248 – 6251; *Angew. Chem. Int. Ed.* **2009**, *48*, 6132 – 6135; b) S. Dang, J. H. Zhang, Z. M. Sun, *J. Mater. Chem.* **2012**, *22*, 8868 – 8873; c) H. B. Zhang, X. C. Shan, L. J. Zhou, P. Lin, R. F. Li, E. Ma, X. G. Guo, S. W. Du, *J. Mater. Chem. C* **2013**, *1*, 888 – 891; d) S. Zhang, D. Du, K. Tan, J. Qin, H. Dong, S. Li, W. He, Y. Lan, P. Shen, Z. Su, *Chem. Eur. J.* **2013**, *19*, 11279 – 11286.

[10] a) B. V. Harbuzaru, A. Corma, F. Rey, J. L. Jordá, D. Ananias, L. D. Carlos, J. Rocha, *Angew. Chem.* **2009**, *121*, 6598 – 6601; *Angew. Chem. Int. Ed.* **2009**, *48*, 6476 – 6479; b) Y. J. Cui, H. Xu, Y. F. Yue, Z. Y Guo, J. C. Yu, Z. X. Chen, J. K. Gao, Y. Yang, G. D. Qian, B. L. Chen, *J. Am. Chem. Soc.* **2012**, *134*, 3979 – 3982.

[11] a) C. M. Kowalchuk, F. A. A. Paz, D. Ananias, P. Pattison, L. D. Carlos, J. Rocha, *Chem. Eur. J.* **2008**, *14*, 8157 – 8168; b) D. F. Sava, L. E. S. Rohwer, M. A. Rodriguez, T. M. Nenoff, *J. Am. Chem. Soc.* **2012**, *134*, 3983 – 3986; c) J. Qin, S. Bao, P. Li, W. Xie, D. Du, L. Zhao, Y. Lan, Z. Su, *Chem. Asian J.* **2014**, *9*, 749 – 753.

[12] a) M. D. Allendorf, C. A. Bauer, R. K. Bhakta, R. J. Houk, *Chem. Soc. Rev.* **2009**, *38*, 1330 – 1352; b) D. P. Yan, G. O. Lloyd, A. Delori, W. Jones, X. Duan, *ChemPlusChem* **2012**, *77*, 1112 – 1118.

[13] J.-S. Qin, D.-Y. Du, W.-L. Li, J.-P. Zhang, S.-L. Li, Z.-M. Su, X.-L. Wang, Q. Xu, K.-Z. Shao, Y.-Q. Lan, *Chem. Sci.* **2012**, *3*, 2114 – 2118.

[14] a) G. S. Yang, Y. Q. Lan, H. Y. Zang, K. Z. Shao, X. L. Wang, Z. M. Su, C. J. Jiang, *CrystEngComm* **2009**, *11*, 274 – 277; b) E. Neofotistou, C. D. Malliakas, P. N. Trikalitis, *CrystEngComm* **2010**, *12*, 1034 – 1037.

[15] A. L. Spek, *J. Appl. Crystallogr.* **2003**, *36*, 7 – 13.

[16] a) H. Li, M. Eddaoudi, M. O'Keeffe, O. M. Yaghi, *Nature* **1999**, *402*, 276 – 279; b) J. Jia, F. Sun, Q. Fang, X. Liang, K. Cai, Z. Bian, H. Zhao, L. Gao, G. Zhu, *Chem. Commun.* **2011**, *47*, 9167 – 9169.

[17] a) G.-G. Hou, Y. Liu, Q.-K. Liu, J.-P. Ma, Y.-B. Dong, *Chem. Commun.* **2011**, *47*, 10731 – 10733; b) J. Cao, Y. Gao, Y. Wang, C. Du, Z. Liu, *Chem. Commun.* **2013**, *49*, 6897 – 6899.

[18] a) J.-S. Qin, D.-Y. Du, L. Chen, X.-Y. Sun, Y.-Q. Lan, Z.-M. Su, *J. Solid State Chem.* **2011**, *184*, 373 – 378; b) D.-Y. Du, J.-S. Qin, C.-X. Sun, X.-L. Wang, S.-R. Zhang, P. Shen, S.-L. Li, Z.-M. Su, Y.-Q. Lan, *J. Mater. Chem.* **2012**, *22*, 19673 – 19678; c) Y.-Q. Sun, J. Zhang, Y.-M. Chen, G.-Y. Yang, *Angew. Chem.* **2005**, *117*, 5964 – 5967; *Angew. Chem. Int. Ed.* **2005**, *44*, 5814 – 5817.

[19] B. Adhikari, G. Palui, A. Banerjee, *Soft Matter* **2009**, *5*, 3452 – 3452.

[20] a) J. T. Jia, F. X. Sun, T. Borjigin, H. Ren, T. T. Zhang, Z. Bian, L. X. Gao, G. S. Zhu, *Chem. Commun.* **2012**, *48*, 6010 – 6012; b) C. M. Doherty, Y. Gao, B. Marmiroli, H. Amenitsch, F. Lisi, L. Malfatti, K. Okada, M. Takahashi, A. J. Hill, P. Innocenzi, P. Falcaro, *J. Mater. Chem.* **2012**, *22*, 16191 – 16195.

[21] a) G. M. Sheldrick, SHELXS-97, *Programs for X-ray Crystal Structure Solution*, University of Göttingen, Germany, **1997**; b) G. M. Sheldrick, SHELXL-97, *Programs for X-ray Crystal Structure Refinement*, University of Göttingen, Germany, **1997**; c) L. J. Farrugia, WINGX, *A Windows Program for Crystal Structure Analysis*, University of Glasgow, UK, **1988**.

Received: November 15, 2013